

Novel Biodegradable Ternary Copolymers *hy*-PEI-*g*-PCL-*b*-PEG: Synthesis, Characterization, and Potential as Efficient Nonviral Gene Delivery Vectors

Xintao Shuai, Thomas Merdan, Florian Unger, Matthias Wittmar, and Thomas Kissel*

Department of Pharmaceutics and Biopharmacy, Philipps-University of Marburg, Ketzerbach 63, D-35032 Marburg, Germany

Received March 27, 2003; Revised Manuscript Received May 13, 2003

ABSTRACT: Diblock copolymers (MPEG-*b*-PCLs) of poly(ϵ -caprolactone) (PCL) and monomethoxyl poly(ethylene glycol) (MPEG) were synthesized by the conventional ring-opening polymerization of ϵ -caprolactone using MPEG as a macroinitiator. The monohydroxy-bearing diblock copolymers were reacted first with maleic anhydride and then with *N*-hydroxysuccinimide (NHS) to yield activated succinimidyl carbonate derivatives that are reactive with the primary amino group. Subsequently, a new class of biodegradable amphiphilic copolymer (*hy*-PEI-*g*-PCL-*b*-PEG) was prepared by grafting the activated PCL-*b*-PEG onto the hyperbranched poly(ethylene imine) (*hy*-PEI). Thermal properties of bulk graft copolymers were investigated using differential scanning calorimetry and thermogravimetric analysis. Depending on their compositions, these polymers are completely soluble in water or form micelles of tens to hundreds of nanometers in size in the studied concentration range, as revealed by surface tension and dynamic light scattering measurements of copolymer solutions. Complexation of plasmid DNA (pDNA) with various copolymers was investigated to achieve particles of ca. 200 nm diameter ($N/P = 7$). Copolymer composition was found to affect significantly the gene transfection efficiency of polyplexes. In general, low graft density and high molecular weight of PEI blocks favor high gene transfection efficiency. All DNA/copolymer complexes ($N/P = 7$) showed a much lower ξ -potential (i.e., neutral or negative) than the DNA/PEI25 kDa complex (21 mV), indicating lower toxicity of copolymer-based complexes. Lower cytotoxicity of DNA/copolymer complexes was also demonstrated by the viability of cells in the transfection experiments. These results indicate that these ternary copolymers are promising candidates for gene delivery, featuring good biocompatibility, potential biodegradability, and relatively high gene transfection efficiency. Their neutral surface charge offers potential for intravenous administration.

Introduction

So far, a number of gene delivery systems of DNA complexes with various polycations have been investigated, including cationic homopolymers such as poly(ethylene imine) (PEI),¹ poly(L-lysine),^{2,3} and poly(amino ester),⁴ dendrimers such as poly(amidoamine) (PAM-AM)⁵ and poly(propylene imine) (PPI),⁶ and cationic block or graft copolymers based on these homopolymers, e.g., poly(ethylene glycol)-*block*-poly(L-lysine).^{7–10} In these systems, DNA compaction and condensation to virus core-like particles suitable for cell uptake are achieved as a result of spontaneous electrostatic interaction between the positively charged groups of polycation and the negatively charged phosphate groups of DNA. Most studies focused on increasing efficiency of transgene expression and improving bioavailability of these polyplexes, while decreasing their toxicity.¹¹

Among synthetic cationic homopolymers for gene delivery, PEI offers the highest positive charge density for strong DNA affinity and exhibits an unique proton-sponge effect over a broad pH range, which allows gene transfer to cytoplasm without co-administration of endosome disruptive reagents.^{12,13} As both PEI and DNA will lose solubility in aqueous media after charge neutralization, sufficient chain length excess of PEI over DNA is essential to generate a soluble cationic corona

of nanoparticles for efficient gene transfer.¹⁴ This means that soluble nano-polyplexes can be produced only with high molecular weight PEI. However, high molecular weight PEI is cytotoxic due to its high positive charge, and PEI/pDNA polyplexes tend to aggregate under physiological conditions.

To overcome these problems, the use of PEI-based copolymers, instead of homo-PEI, to form DNA complexes has been extensively studied recently.^{14–19} Most studies utilized nonionic hydrophilic polyethers, such as poly(ethylene glycol) (PEG), as building block to synthesize block or graft copolymers with either linear or hyperbranched PEIs. When these copolymers were mixed with p-DNA in aqueous solution, the cationic PEI segments of copolymers were first bound to DNA via electrostatic interaction and then the neutralized polyions aggregated to form an insoluble core, while the nonionic water-soluble PEG chains served as a hydrophilic shell stabilizing the nanoparticles.¹⁴ Complexes thus prepared are less positively charged or neutral and therefore are potentially less toxic. Indeed, DNA nano-complexes with copolymers of PEI and PEG showing transgene expression and enhanced biocompatibility have been successfully obtained. However, one drawback for the in vivo application of these copolymers is their lack of biodegradability, since PEI and PEG were coupled by urethane,¹⁴ urethane and urea,^{17–19} or other bonds,¹⁶ which are very stable against hydrolysis under physiological conditions. It is well-known that only hydrophilic low molecular weight substances with mo-

* To whom correspondence should be addressed: Tel +49-6421-282-5881; FAX +49-6421-282-7016; e-mail kissel@mail.uni-marburg.de.

lecular weights < 30 kDa can be eliminated by the kidney, and high molecular weight polymers used for drug delivery must be degraded or metabolized before they can be eliminated.²⁰ Consequently, in vivo use of nonbiodegradable polycations of high molecular weights (e.g., >30 kDa) for gene therapy may inevitably result in accumulation of polymers in the human body and may cause severe organ damage. In the present study, we synthesized a new type of ternary copolymer by grafting diblock copolymers of PEG and PCL onto *hy*-PEIs with molecular weights < 30 kDa. We investigated the feasibility of using these copolymers to design more desirable gene delivery systems in terms of gene transfection efficiency and cytotoxicity. We believe that DNA delivery systems based on copolymers of PEI and PEG linked to a readily biodegradable polyester might be more desirable for in vivo applications due to their biodegradability.

Moreover, hydrophobic moieties incorporated into the gene delivery vectors are believed to enhance cell interactions and tissue permeability of delivery systems. For instance, copolymers of poly(ethylene oxide) and poly(propylene oxide) (PPO) were found to possess the unique ability of incorporating into cell membranes as a result of the presence of the hydrophobic PPO chain.²¹ Kabanov et al. recently reported gene delivery polyplexes based on Pluronic-*graft*-poly(ethylene imine)s.²² In addition, Mahato et al. recently reported delivery systems based on amphiphilic lipopolymers, branched poly(ethylene imine)-*graft*-cholesterols, in the hope that the lipid coating on the DNA may increase the permeability of complexes through cell membranes.²³ In light of these results, we speculated that incorporation of hydrophobic polyester moieties in a delivery system might have a similar promoting effect on gene transport into cells. The work reported here is a result of our long-standing effort to develop gene delivery systems possessing good biocompatibility, potential biodegradability, and high gene transfection efficiency.²⁰

Experimental Section

Materials. ϵ -Caprolactone (from Aldrich) was purified by vacuum distillation over CaH_2 . Toluene was dried by refluxing over sodium and distilled under dry argon. MPEGs with various molecular weights (from Aldrich) were first purified by precipitation into hexane from tetrahydrofuran (THF), and then the vacuum-dried precipitates were further dried by azeotropic distillation with dry toluene. *hy*-PEIs with molecular weights of 800, 2000, and 25 000 Da were gifts from BASF and were used as received. The ratio of primary, secondary, and tertiary amino groups of *hy*-PEIs was determined as previously discussed.¹³ Stannous(II) octoate (SnOct), maleic anhydride, dicyclohexylcarbodiimide (DCC), and *N*-hydroxysuccinimide (NHS) were all from Aldrich and were used as received.

pCMV-Luc encoding for luciferase as a reporter gene was purchased from Plasmid Factory, Bielefeld, Germany. NIH/3T3 (Swiss mouse embryo) cell line was purchased from the German Collection of Microorganisms and Cell Cultures (DSMZ, Braunschweig, Germany). Cells were cultured according to the protocols suggested by the supplier.

Synthesis of Monohydroxy-Terminated Diblock Copolymers of PCL and MPEG. Monohydroxy-terminated diblock copolymers were synthesized by ring-opening polymerization of ϵ -caprolactone using MPEG as a macroinitiator and SnOct as a catalyst.²⁴ ϵ -CL, SnOct (ca. 0.1% of ϵ -CL in molar amount), and MPEG were weighed into a round-bottomed flask equipped with a magnetic stirring bar. The flask was sealed under dry argon and was immersed in an oil bath at 115 °C for 24 h. The product was purified, by twice

precipitating into cold methanol from dichloromethane (DCM) solution, and was then vacuum-dried at 40 °C. The degree of polymerization of the PCL block was calculated by comparing integrals of characteristic peaks of the PCL block at ~2.25 ppm (triplet, $-\text{C}(=\text{O})-\text{CH}_2-$) and PEG block at 3.35 ppm (singlet, $-\text{OCH}_2-$) in the ^1H NMR spectrum. The molecular weight and polydispersity of diblock copolymers were also estimated by GPC measurements. MPEG-*b*-PCL-OH yields: >95%.

Synthesis of Monocarboxy-Capped Diblock Copolymers. This can be accomplished by hydroxyl esterification with either succinic or maleic anhydride, according to a similar method reported previously for esterification of monohydroxy-terminated PEG (MPEG-OH).^{25,26} Maleic anhydride was chosen in the present research because it has been demonstrated to be more reactive in the MPEG-OH esterification,²⁶ and it is easy to eliminate via sublimation after the esterification. Typically, monohydroxy-terminated diblock copolymer (0.5 mmol) and maleic anhydride (1 mmol) were dissolved in dry toluene (15 mL) and placed in a two-necked flask equipped with a magnetic stirring bar and a reflux condenser. Pyridine (1 mmol) was added to the flask, and the mixture under a dry argon atmosphere was stirred at 70 °C for 48 h. Crude polymer obtained by precipitation into cold hexane was redissolved in DCM. The DCM solution was washed three times with aqueous hydrochloric acid (10% in v/v) and then four times with a saturated NaCl solution. Then the organic phase was isolated, dried over magnesium sulfate, and filtered. Polymer recovered by precipitation into cold hexane was vacuum-dried to a constant weight at 50 °C to eliminate any water and maleic anhydride residues. MPEG-*b*-PCL-COOH yields: >92%.

Synthesis of Amino-Group-Reactive Succinimidyl Carbonate of Diblock Copolymer. This reaction was performed in a way similar to preparing activated succinimidyl carbonates based on carboxy-capped PEG derivatives.^{27,28} Monocarboxy-capped diblock copolymer (0.54 mmol) and NHS (2.7 mmol) were dissolved in DCM (20 mL) and placed in a flask equipped with a magnetic stirring bar. The flask was cooled in an ice-water bath, and DCC (2.7 mmol) was added. The reaction mixture was sealed under argon and was stirred at 0 °C for 1 h and at room temperature for 24 h. The precipitated 1,3-dicyclohexylurea (DCU) was removed by filtration. The filtrate was added to diethyl ether (50 mL) and cooled at 4 °C for 2 h. The precipitate, a white oily, waxy, or powdery solid depending on the composition of diblock copolymer, was collected by filtration, washed with 2-propanol, and finally dried under vacuum at room temperature. Nonaqueous alkaline titration^{26,27} in a 1/3 (v/v) mixture of methanol and THF indicates that, for all activated samples, the free carboxylic group was less than 3.7% of the initial total detected before activation. MPEG-*b*-PCL-NHS yields: 82–97%.

Conjugation of Activated Diblock Copolymers onto *hy*-PEIs. The predetermined amount, according to the molecular design, of *hy*-PEI (e.g., 0.50 g) and activated diblock copolymer (e.g., 0.5 g) were dissolved in DCM (e.g., 15 mL, volume was set according to the amount of reactants) in a glass vial, sealed under argon, and magnetically stirred for 24 h at room temperature. Crude copolymer collected by precipitation into diethyl ether (e.g., 200 mL) and filtration was redissolved in DCM and dialyzed against pure DCM to remove possibly unreacted PEI and diblock copolymer. The purified graft copolymer was recovered by the rotary evaporation of solvent under reduced pressure and dried under vacuum at room temperature (yields: 57–89%).

Characterization of Polymers. Polymer structures were characterized with Fourier transform infrared (FTIR) and nuclear magnetic resonance (NMR) spectroscopies. FTIR spectral studies were carried out with a Nicolet 510P FTIR spectrometer in the range between 4000 and 750 cm^{-1} , with a resolution of 2 cm^{-1} . All powder samples were compressed into KBr pellets for the FTIR measurements. NMR spectra were recorded on a JEOL GX 400 D spectrometer in CDCl_3 or D_2O at room temperature.

Gel permeation chromatography (GPC) was employed to determine the molecular weight and the molecular weight distribution. GPC analysis was carried out using a SDV Linear

M 5 μ 8 \times 300 mm column (Polymer Standard Service, Mainz, Germany) with DCM as an eluent (1 mL/min) and polystyrene standards for column calibration. 20 μ L samples were injected with a Merck Hitachi autosampler AS-2000A. The eluent was analyzed with a differential refractive index (RI) detector RI-71 from Merck and an 18 angle laser light scattering detector from Wyatt Technologies (DAWN EOS, GaAs laser 690 nm, 30 mW, K5 cell).

DSC measurements were performed at a heating rate of 10 $^{\circ}$ C/min on a Perkin-Elmer differential scanning calorimeter (DSC-7) calibrated with indium and gallium. TGA was conducted on a Perkin-Elmer thermogravimetric analyzer TGA 7 with a thermal analysis controller at a heating rate of 20 $^{\circ}$ C/min.

Determination of Critical Micellization Concentration. The critical micellization concentration (cmc) was evaluated using the surface tension method.^{29,30} Surface tension of polymer solutions was recorded with a LAUDA MGW tensiometer (Germany) at 25 $^{\circ}$ C.

Polyplex Formation at N/P 3, 7, and 20. Luciferase plasmid (pCMV-luc) and the appropriate amount of polymer were dissolved separately in 0.9% sodium chloride solution at pH = 7. The two solutions were mixed by vigorous pipetting, and complexes were allowed to interact for 10 min before use. Polyplexes were prepared for transfection experiments with 4 μ g plasmid in 300 μ L of NaCl (0.9%) and the appropriate amount of polymer or conjugate in 300 μ L of sodium chloride solution (0.9%, pH = 7).

Photon Correlation Spectroscopy. Hydrodynamic diameters of the DNA/polymer complexes were determined by photon correlation spectroscopy. 4 μ g of pCMV-Luc plasmid was complexed with the appropriate amount of polymer in 50 μ L of sodium chloride solution as described above. Measurements were performed on a Zetasizer 3000 HS from Malvern Instruments, Herrenberg, Germany (10 mW HeNe laser, 633 nm). Scattered light was detected at a 90 $^{\circ}$ angle through a 400 μ m pinhole at a temperature of 25 $^{\circ}$ C. For data analysis, the viscosity (0.88 mPa s) and the refractive index (1.33) of distilled water at 25 $^{\circ}$ C were used. The instrument was routinely calibrated using Standard Reference latex particles (AZ 55 Electrophoresis Standard Kit, Malvern Instruments). Measurements were analyzed by CONTIN algorithm. Values given are the means of five runs of 60 s \pm standard deviation.

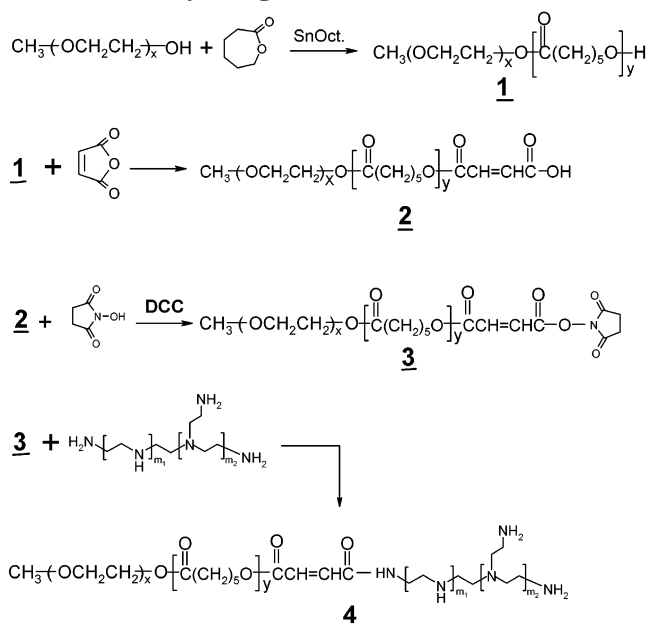
Zeta-Potential Measurements. 16 μ g of pCMV-Luc plasmid was complexed with the appropriate amount of polymer in 800 μ L of NaCl (150 mM) as described above. Zeta-potential measurements of polyplexes formed at N/P 7 were carried out in the standard capillary electrophoresis cell of the Zetasizer 3000 HS from Malvern Instruments at position 17.0 at 25 $^{\circ}$ C. The sampling time was set to automatic. Average values were calculated with the data from five runs.

Transfection Experiments. Transfection experiments were performed with 4 μ g of pCMV-Luc. NIH/3T3 cells were seeded in 12 well plates at a density of 50 000 cells per well. After 24 h, the medium was removed and complexes were added in 1.5 mL of fresh media. Media was exchanged again after 4 h, and cells were incubated for a further 44 h. Luciferase gene expression was quantified using a commercial kit (Promega) and photon counting with a luminometer (Sirius, Berthold). Results in relative light units per second (RLU/s) were converted into nanograms of luciferase by creating a calibration curve with recombinant luciferase (Promega). Protein concentration in each sample indicating cell viability was determined using a BCA assay.³¹ All experiments were performed in triplicate, and data were expressed in nanograms of luciferase per milligram of protein.

Results and Discussion

Synthesis of *hy*-PEI-*g*-PCL-*b*-PEGs. Recently, we reported^{17,18} the successful grafting of hydroxy-terminated PEGs onto *hy*-PEIs using an aliphatic diisocyanate, e.g., hexamethylene diisocyanate (HMDI), as a coupling reagent. DNA/PEI-*g*-PEG polyplexes with en-

Scheme 1. Synthetic Approach to *hy*-PEI-*g*-PCL-*b*-MPEG



hanced biocompatibility and gene delivery efficacy compared to DNA/PEI polyplexes were obtained by controlling the graft density and molecular weights of PEI and PEG in the synthesis of *hy*-PEI-*g*-PEGs. Despite its high reactivity with both hydroxyl and amino groups, aliphatic diisocyanates were not used here to couple the $-NH_2$ -bearing PEI and the hydroxy-terminated diblock copolymer for two reasons. First, to avoid coupling reaction between two HO-terminated copolymer molecules, a large excess of diisocyanate is required, which however must be thoroughly removed before the coupling reaction with *hy*-PEIs, because even a small amount of residual diisocyanate may result in inter- and intramolecular cross-linking of *hy*-PEIs and lead to insoluble graft copolymers. Second, the isocyanated prepolymers may react with water and lose reactivity, therefore requiring purification of activated prepolymers conducted carefully under anhydrous conditions (e.g., dry solvents and isolation of humidity), and *hy*-PEI must be dried prior to use. In the present research, synthesis of *hy*-PEI-*g*-PCL-*b*-MPEGs was carried out using a different approach, which has been usually adopted to couple PEGs onto peptides and proteins²⁸ and in which intra-prepolymer coupling was completely avoided, as shown in Scheme 1. The composition, i.e., block contents and graft density, of *hy*-PEI-*g*-PCL-*b*-MPEG was manipulated by preselecting commercially available MPEGs and PEIs of known molecular weights and controlling the feed amount of ϵ -CL. Spectrometric methods were employed to characterize diblock intermediates (i.e., hydroxy-, carboxy-, and NHS-terminated copolymers) and *hy*-PEI-*g*-PCL-*b*-MPEGs. Figure 1 shows the FTIR spectra of the diblock intermediates and a corresponding graft copolymer. PCL and PEG blocks were characterized by prominent absorptions at ~ 1726 cm^{-1} (s, $\nu_{C=O}$) and 1105 cm^{-1} (s, ν_{C-O}), respectively. Obviously, both PCL and PEG blocks are present in all three intermediate prepolymers and the final graft copolymer. A strong absorption of the incorporated maleic segment at ~ 1635 cm^{-1} (s, $\nu_{C=C}$), which is absent in the spectrum of the hydroxy-terminated prepolymer, was observed for both carboxy- and NHS-terminated prepolymers but was overlapping with the amide absorption (s, $\nu_{C=O}$) in

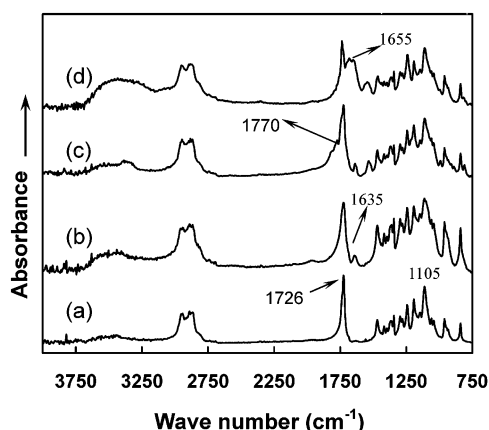


Figure 1. FTIR spectra of HO-terminated MPEG2000-*b*-PCL1200 (a), carboxy-terminated MPEG2000-*b*-PCL1200 (b), NHS-terminated MPEG2000-*b*-PCL1200 (c), and PEI25K-*g*-(PCL1200-*b*-PEG2000)_{5.1} (d).

spectrum d of the graft copolymer. The absorption around 1770 cm⁻¹ partially overlapping with the ester absorption was assigned to the succinimidyl end group (s, $\nu_{\text{imide,C=O}}$) in spectrum c of NHS-terminated prepolymer. This peak disappeared, and a new and strong absorption around 1655 cm⁻¹ attributed to the amide linkage (s, $\nu_{\text{amide,C=O}}$) appeared in the spectrum of graft copolymer. It was noted that graft copolymers of higher graft density showed stronger amide absorptions. In addition, the graft copolymer showed strong and broad

characteristic absorption of amines around 3300 cm⁻¹ (s, $\nu_{\text{N-H}}$). These FTIR results are consistent with the expected structures of intermediate prepolymers and graft copolymers.

¹H NMR spectra of a graft copolymer and corresponding intermediate prepolymers are shown in Figure 2. ¹H NMR resonance signals of MPEG-*b*-PCL-OH are fully attributed, as shown in Figure 2a. The characteristic resonances of both PCL and MPEG were observed also in Figure 2b–d, indicating the coexistence of two blocks in the carboxy- and NHS-terminated prepolymers as well as in the graft copolymer. Prepolymers and graft copolymer showed two resonance signals at ~6.4 ppm (doublet, -C(=O)CH=CHC(=O)-), which are not present in the spectrum of MPEG-*b*-PCL-OH containing no maleic moiety. In addition, the NHS-activated prepolymer showed a signal at ~2.85 ppm (singlet, 4H, NHS protons), while the graft copolymer showed strong and broad absorption at ~2.65 ppm (multiplet, methylene protons of *hy*-PEI). These results are in line with the results obtained in the FTIR measurements and demonstrated the successful synthesis of intermediate prepolymers and graft copolymers. From ¹H NMR spectra, the PCL length and graft density of copolymer were calculated from the integral values of characteristic peaks of PEG (e.g., CH₃O- at ~3.38 ppm), PCL (e.g., -C(=O)-CH₂- at ~2.3 ppm), and PEI (-CH₂CH₂- at ~2.65 ppm), using the known molecular weight of MPEG and PEI. It is noteworthy that the method of comparing integration of ¹H NMR peaks was also used

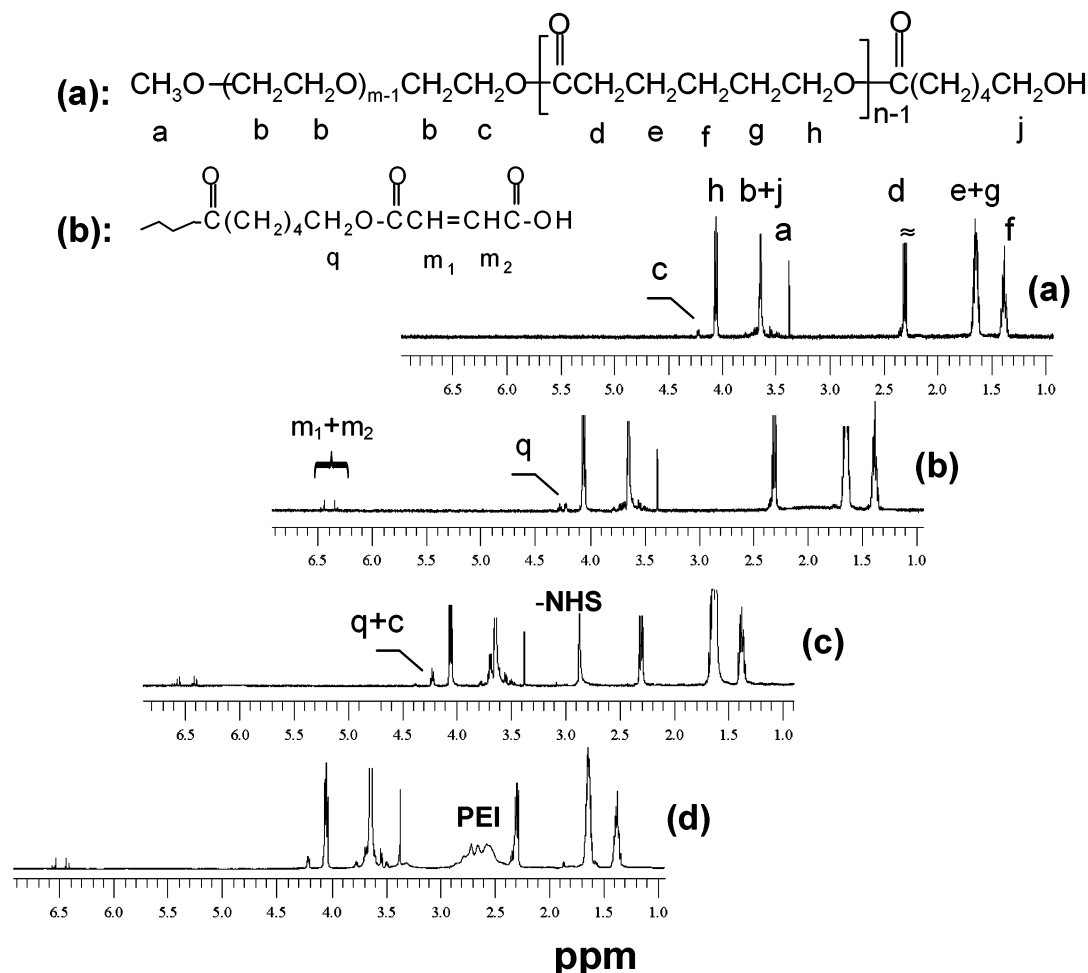


Figure 2. ¹H NMR spectra of HO-terminated MPEG2000-*b*-PCL1200 (a), COOH-terminated MPEG2000-*b*-PCL1200 (b), NHS-terminated MPEG2000-*b*-PCL1200 (c), and PEI25K-*g*-(PCL1200-*b*-PEG2000)_{5.1} (d), in CDCl₃.

Table 1. Copolymer Composition and Thermal Properties

| copolymer ^a | PEI content ^a (%) | PCL content ^a (%) | <i>T</i> _g ^b (°C) | <i>T</i> _m ^b (°C) | <i>M</i> _n ^d (10 ⁴) | <i>M</i> _w / <i>M</i> _n ^d |
|---|------------------------------|------------------------------|---|---|---|--|
| PEI800- <i>g</i> -(PCL1200PEG2000) _{1.4} | 15 | 32 | nd ^c | 54.07 | 0.60 | 1.2 |
| PEI800- <i>g</i> -(PCL3800PEG5000) _{1.1} | 8 | 40 | nd ^c | 51.35 | 1.06 | 1.1 |
| PEI2000- <i>g</i> -(PCL580PEG5000) _{2.2} | 14 | 9 | nd ^c | 54.97 | 1.60 | 1.6 |
| PEI25K- <i>g</i> -(PCL550PEG550) _{2.1} | 52 | 24 | 14 | nd ^c | 4.57 | 1.5 |
| PEI25K- <i>g</i> -(PCL580PEG5000) _{2.9} | 61 | 4 | 4.4 | 54.79 | 4.17 | 1.4 |
| PEI25K- <i>g</i> -(PCL1200PEG2000) _{5.1} | 61 | 15 | nd ^c | 47.84 | 3.89 | 2.7 |
| PEI25K- <i>g</i> -(PCL2000PEG2000) _{2.8} | 69 | 15 | -8 | 46.02 | 3.58 | 1.5 |
| PEI25K- <i>g</i> -(PCL3800PEG5000) _{1.4} | 67 | 14 | -13 | 41.83 | 3.39 | 1.8 |
| PEI25K- <i>g</i> -(PCL3800PEG5000) _{2.6} | 52 | 21 | -6.5 | 52.05 | 4.89 | 2.4 |
| PEI25K- <i>g</i> -(PCL3800PEG5000) _{4.5} | 39 | 26 | 2.1 | 53.14 | 7.12 | 1.6 |

^a Calculated based on ¹H NMR spectra. ^b From the second heating run DSC measurements. ^c Not found. ^d GPC data.

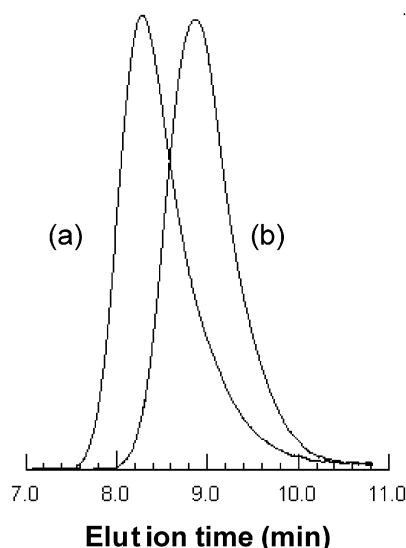


Figure 3. GPC eluograms of PEI25K-*g*-(PCL2000-*b*-PEG-2000)_{2.8} (a) and HO-terminated MPEG2000-*b*-PCL2000 (b).

by several authors^{16,17} to determine the ratio of PEG and PEI segments, i.e., the graft densities, of *hy*-PEI-*g*-PEGs. The graft densities of *hy*-PEI-*g*-PCL-*b*-MPEGs calculated from ¹H NMR spectra, as summarized in Table 1, are in reasonable agreement with those calculated from the amount of PEI in the feed (data not shown) as well as by GPC measurements.

Furthermore, GPC measurements were employed to verify the successful synthesis of intermediate prepolymers and graft copolymers. Prepolymers and graft copolymers after purification all showed unimodal molecular weight distribution in the GPC eluograms, as illustrated in Figure 3, indicating no or negligible homopolymer residue in the copolymer products. Molecular weights of graft copolymers estimated by GPC measurements (Table 1) are close to those calculated from ¹H NMR spectra, especially for copolymers synthesized with low molecular weight *hy*-PEIs.

Thermal Properties and Water Solubility. With TGA measurements, the temperatures of thermal decomposition (*T*_d) of MPEGs and *hy*-PEIs have been studied, and the molecular-weight-dependent decomposition behavior has been revealed in our recent work.¹⁷ Briefly, MPEG (*M*_n = 550, 2000, and 5000) decomposed at ~250–280 °C, whereas decomposition of *hy*-PEIs (*M*_n = 800, 2000, and 25 kDa) was observed at higher temperatures (~330–380 °C). For both homopolymers, higher molecular weight resulted in higher *T*_d. TGA thermograms of a diblock copolymer and a graft copolymer based on MPEG 2000, PCL1200, and PEI25 kDa are shown in Figure 4. Obviously, the weight-loss transition of PEG blocks in MPEG-*b*-PCL-OH was

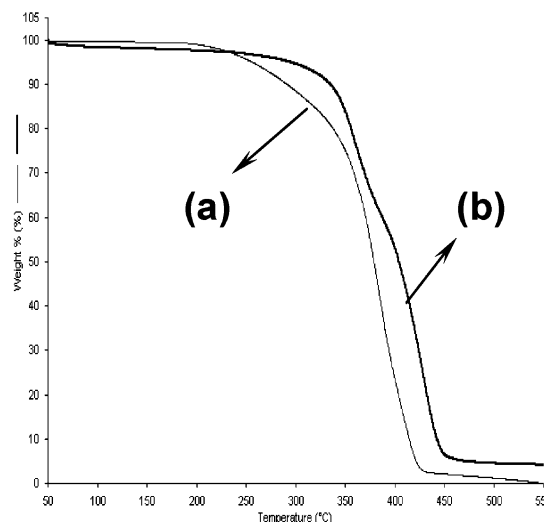


Figure 4. TGA scans of HO-terminated MPEG2000-*b*-PCL1200 (a) and PEI25K-*g*-(PCL1200PEG2000)_{5.1} (b).

partially overlapping with that of PCL blocks which appears to decompose at ~340 °C,³² almost the same *T*_d as low molecular weight PEI. Only two distinct thermal decomposition transitions, instead of three, beginning at 330 and 370 °C are clearly seen in the TGA thermogram of the graft copolymer, corresponding apparently to the *T*_d's of PCL and PEI segments, respectively. Further, *T*_d of independent MPEG (<300 °C) was not detected. The thermal decomposition behavior of this graft copolymer is however not completely out of our expectation since we also found similar results in the TGA measurements of *hy*-PEI-*g*-MPEGs.¹⁷ Depending on the constitutions of *hy*-PEI-*g*-MPEGs, even a single thermal decomposition behavior was frequently observed in that work.

Depending on its constitution, i.e., block length and graft density, *hy*-PEI-*g*-PCL-*b*-MPEG has also been found very frequently to show only a single *T*_d. Two reasons may be given for this unimodal thermal decomposition behavior of some *hy*-PEI-*g*-PCL-*b*-MPEGs as well as *hy*-PEI-*g*-MPEGs prepared in our previous work. First, overlapping of PEI, PCL, and PEG block *T*_d's is possible considering the relatively high heating rate (20 °C/min). Second, it is known that miscibility enhancement in block copolymer bulk materials or polymer blends may also lead to the identical component *T*_d's,^{32,33} and it is noteworthy that block copolymerization has been reported to enhance miscibility of blocks.³⁴ Indeed, in comparison with physical blends, enhanced miscibility was verified by DSC measurements in *hy*-PEI-*g*-MPEGs as reported previously and also in *hy*-PEI-*g*-PCL-*b*-MPEGs as will be discussed below.

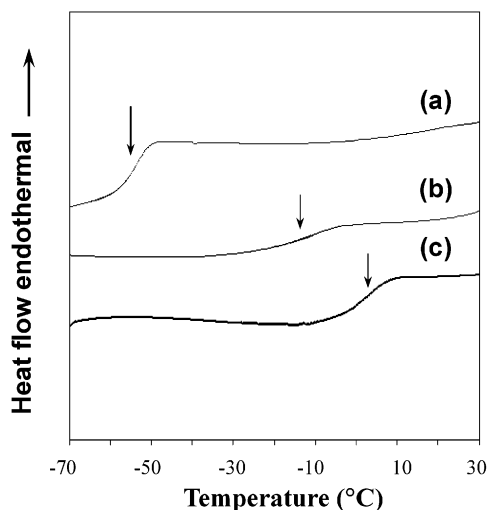


Figure 5. Second heating run DSC thermograms of physical blend (1:1 in weight) of PEI25 kDa and hydroxy-capped MPEG3800-*b*-PCL5000 (a), PEI25K-*g*-(PCL2000PEG2000)_{2.8} (b), and PEI25K-*g*-(PCL3800PEG5000)_{4.5} (c).

In the DSC measurements, unfortunately we failed to detect accurate T_g 's of MPEG and *hy*-PEI because PEG crystallized too quickly and thus did not show a clear glass transition, and *hy*-PEI absorbed water easily during the sample preparation, resulting in shifting T_g 's. The composition-dependent T_g 's were observed in the second-run DSC scans for most graft copolymers; the data should be reliable because these graft copolymers are less sensitive to water, and thus their T_g 's were much less affected by tiny amounts of residual water, even if present, in the vacuum-dried samples. Indeed, unlike its PEI homopolymer counterpart, the graft copolymer exhibited a quite constant T_g in several parallel measurements. The second heating run DSC thermograms of three graft copolymers of different compositions are shown in Figure 5. In general, a T_g shift to higher values was observed with increasing the graft chain length as well as the graft density. This indicates that the graft copolymer bulk phase might be at least a partially miscible system. Although *hy*-PEI and PEG were found to be immiscible, enhanced miscibility in their graft copolymer was detected in our previous work. This is consistent with the report by Jedlinski et al. that block copolymerization of two immiscible polyesters, i.e., α -PHB and PCL, resulted in at least a partially miscible copolymer.³⁴ The possible hydrogen bonding between MPEG and PEI blocks might lead to the enhanced miscibility as well as the physical cross-linking, resulting in loss of chain mobility and high T_g values in DSC measurements of *hy*-PEI-*g*-MPEGs.¹⁷ *hy*-PEI-*g*-PCL-*b*-MPEG contains polyester segments that apparently form hydrogen bonding with amines more readily than PEG. To clarify the possible hydrogen bonding between PEI and PCL segments, we used FTIR spectroscopy, which is known to be a particularly suitable technique to investigate the interpolymer hydrogen bonding between hydroxyl-bearing components and polyester.³⁵ The expanded $\nu_{C=O}$ absorption band of the semicrystalline PCL is very indicative for the PCL phase structure in the FTIR measurements.^{36,37} Figure 6 shows the expansion of carbonyl absorption bands of a MPEG-*b*-PCL-OH and two typical *hy*-PEI-*g*-PCL-*b*-MPEGs, which provides helpful information on hydrogen bonding and the phase structure of PCL blocks. For the diblock copolymer (a), the carbonyl absorption

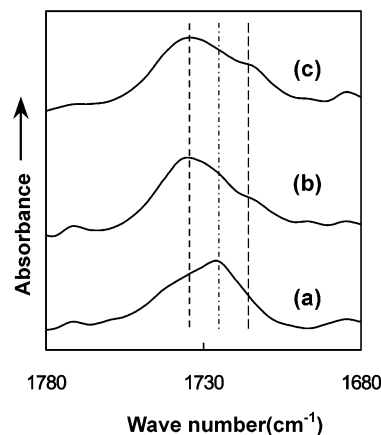


Figure 6. FTIR spectra of hydroxy-capped MPEG5000-*b*-PCL3800 (a), PEI25K-*g*-(PCL3800-*b*-PEG5000)_{1.4} (b), and PEI25K-*g*-(PCL3800-*b*-PEG5000)_{4.5} (c).

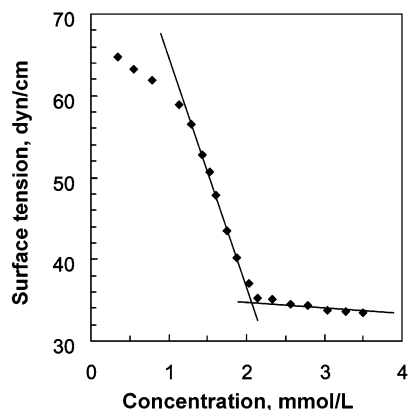
($\nu_{C=O}$) band of PCL blocks is well resolved into two bands corresponding to crystalline ($\sim 1725\text{ cm}^{-1}$) and amorphous ($\sim 1736\text{ cm}^{-1}$) absorptions. The absorption of the crystalline phase is much stronger than that of the amorphous one which appears as a shoulder, suggesting high PCL crystallinity in the diblock copolymers. Upon grafting onto *hy*-PEIs, the absorption of crystalline PCL at 1725 cm^{-1} becomes weak, while the absorption of the amorphous PCL at 1736 cm^{-1} appears as the main peak, as shown in spectra b and c. These results indicate that the crystallization of PCL blocks has been significantly suppressed in the graft copolymers. Moreover, a new peak at $\sim 1715\text{ cm}^{-1}$ appears as a prominent shoulder in the graft copolymers, and its intensity is correlated with the copolymer composition. It is known that, in the FTIR measurements, stretching absorption bands of hydrogen-bonded carbonyl groups always shift to lower frequency.³⁵ Therefore, it is reasonable to assume that this new absorption at $\sim 1715\text{ cm}^{-1}$ results from the PCL carbonyl groups that are hydrogen-bonded to the amino groups of PEI. We believe that the hydrogen bonding between PCL and PEI contributed significantly to the enhanced miscibility of the graft copolymers and in some extreme cases may cause intensive inter- and intramolecular cross-linking and thus result in significant shifts of T_g toward higher values. Indeed, we have noted that it needed great efforts (e.g., long time and elevated temperature) to dissociate the bulk graft copolymers in water.

Depending on their compositions, the graft copolymers dissolved in water were found to be completely soluble at the molecular level or just formed micelles in certain concentration ranges. The aqueous association of graft copolymers was investigated by surface tension and hydrodynamic size measurements. A typical change of surface tension with copolymer concentration is shown in Figure 7. The surface tension of this copolymer solution first diminished with increasing concentration and started to level off at a copolymer concentration of 2.07 mmol/L. Therefore, we assume that 2.07 mmol/L is the cmc of this copolymer.^{29,30} The cmc's of various copolymers obtained by this method are summarized in Table 2. It is noteworthy that a clear cmc was not detectable for some graft copolymers containing high molecular weight PEI and short PCL blocks. In this case, we believe that the short PCL chains have not been able to aggregate and affect the solubility of copolymers at least in the investigated concentration range. For the

Table 2. Copolymer Solubility in Water, Their DNA Complex Size, and ξ -Potential at N/P 7

| composition | copolymer | | complex | |
|---|---------------------------|----------------------------|------------------------------------|------------------------------------|
| | cmc ^a (mmol/L) | <i>D</i> ^b (nm) | size ^b (nm) (\pm SD) | ξ -potential ^b (mV) |
| PEI800 | nd ^c | nd ^c | 320.5 \pm 15.9 | -16.4 \pm 7.3 |
| PEI25K | nd ^c | nd ^c | 164.6 \pm 5.4 | 20.9 \pm 2.7 |
| PEI800- <i>g</i> -(PCL1200PEG2000) _{1.4} | 2.07 | 126 | 188.9 \pm 8.4 | -2.7 \pm 0.4 |
| PEI800- <i>g</i> -(PCL3800PEG5000) _{1.1} | 0.024 | 194 | nc ^e | nc ^e |
| PEI2000- <i>g</i> -(PCL580PEG5000) _{2.2} | nd ^c | nd ^c | nc ^e | nc ^e |
| PEI25K- <i>g</i> -(PCL550PEG550) ₂₁ | 0.311 | 96 | 335.5 \pm 15.1 | -10.5 \pm 2.3 |
| PEI25K- <i>g</i> -(PCL580PEG5000) _{2.9} | nd ^c | nd ^c | 207.8 \pm 6.2 | -0.4 \pm 1.9 |
| PEI25K- <i>g</i> -(PCL1200PEG2000) _{5.1} | <0.012 | 253 | 208.4 \pm 8.6 | -3.0 \pm 0.9 |
| PEI25K- <i>g</i> -(PCL2000PEG2000) _{2.8} | 0.031 | 77 | 234.4 \pm 9.8 | -3.5 \pm 0.3 |
| PEI25K- <i>g</i> -(PCL3800PEG5000) _{1.4} | 0.035 | 107 | nc ^e | nc ^e |
| PEI25K- <i>g</i> -(PCL3800PEG5000) _{2.6} | ns ^d | ns ^d | nc ^e | nc ^e |
| PEI25K- <i>g</i> -(PCL3800PEG5000) _{4.5} | ns ^d | ns ^d | nc ^e | nc ^e |

^a Determined with surface tension measurements. ^b Detected with dynamic light scattering. ^c Soluble in experimental range. ^d Failed to dissociate large particles. ^e Complex was not prepared.

**Figure 7.** Surface tension vs concentration of PEI800-*g*-(PCL1200-*b*-PEG2000)_{1.4} in water (25 °C).

copolymers showing a cmc, dynamic light scattering was used to determine the particle size (Table 2) and size distribution. Micelle size is affected significantly by the composition of the graft copolymer studied herein and may vary from tens to hundreds of nanometers.

Polymer–DNA Complexes. Complexes were formed at N/P 3, 7, and 20, which were chosen on the basis of our experiences with DNA/*hy*-PEI-*g*-PEG complexes,¹⁸ and the particle size and ξ -potential of various pDNA/copolymer complexes formed at a N/P ratio of 7 were detected in order to gain first insight into the effect of copolymer composition on the DNA complexation and condensation. It is noteworthy that both particle size and ξ -potential are not indicative of the complex composition. However, it is well-known that particle nano-size is a key prerequisite for cell uptake,²² and ξ -potential correlates to the cytotoxicity of the complexes. Though that polycation excess was found not to incorporate into the complexes in the complexation of oligonucleotides and *hy*-PEI-*g*-PEGs at least up to N/P 3,¹⁴ in many cases a high N/P ratio (>1) has proven to be an essential for efficient DNA complexation and condensation no matter which PEI homo- or copolymers were used.¹⁸ Indeed, as we already pointed out in the Introduction section, PEI excess is an essential (namely N/P > 1) in order to form stable core-shell nanocomplexes of DNA and high molecular weight homo-PEIs. To the complexes formed in the present work, we are interested in the probable influence of N/P ratio on the complex composition. However, this is far beyond the purpose and scope we would like to reach in this paper and therefore is not discussed here.

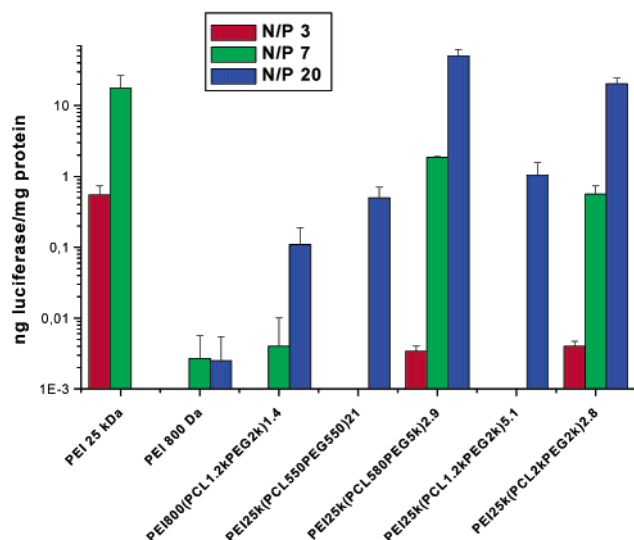
As shown in Table 2, homo-PEI25 kDa formed the smallest stable particles of ca. 160 nm in diameter, indicating the best compaction and condensation of DNA molecules with the high molecular weight PEI. On the contrary, PEI800 Da formed unstable large particles with an initial diameter of ca. 320 nm, indicating poor complexation between DNA and low molecular weight PEI due to the loss of solubility after the interpolyelectrolyte neutralization.¹⁴ Most polyplexes prepared with copolymers showed quite similar sizes around 200 nm. Since all polyplexes were prepared with a control of polymer solution below its micellization concentration, the particle size should be dependent only on the complexation between DNA and polymer. Indeed, as shown in Table 2, the complex size does not correlate obviously with the micelle size of the corresponding copolymer. For instance, polyplex based on PEI25K-*g*-(PCL2000-*b*-PEG2000)_{2.8} is much larger than its polymeric micelle (234 nm vs 77 nm), while polyplex based on PEI25K-*g*-(PCL1200-*b*-PEG2000)_{5.1} is even smaller than its polymeric micelle (208 nm vs 253 nm). It is noteworthy that PEI25K-*g*-(PCL550-*b*-PEG550)₂₁ possessing a quite small micelle size (96 nm) formed the largest particle (335 nm). Note also that this copolymer has the highest graft density; i.e., 21 short chains were grafted onto each PEI molecule on average. In this case, we believe that the dense hydrophobic PCL chains surrounding the PEI head may strongly hinder the access and binding of DNA to PEI and lead to an insufficient compaction and condensation of DNA at this N/P ratio. This becomes apparent when comparing the PEI25K-*g*-(PCL550-*b*-PEG550)₂₁ and PEI800-based complexes that exhibited the closest values of size and ξ -potential, and the latter is well-known to only form loose and unstable complexes with DNA as already mentioned.

As expected, the ξ -potential of the complex based on PEI25 kDa is very high (21 mV), suggesting high positive charge on the particle surface. In contrast, PEI800 Da and all copolymers formed complexes with negatively charged surfaces. Similar results were also found in our recent study with the DNA/PEI-*g*-PEG complexes at relatively high N/P ratios. The same reason can be given as that the shielding effect of neutral components on the copolymer PEI head has led to the lower ξ -potentials of the copolymer-based DNA complexes.¹⁸ Except for PEI25K-*g*-(PCL550-*b*-PEG550)₂₁, other copolymers formed DNA complexes of ξ -potential close to zero. In particular, the PEI25K-*g*-(PCL580-*b*-PEG5000)_{2.9}-based polyplex possesses a neutral surface

Table 3. 3T3 Cell Viability in the Transfection with DNA Polyplexes Based on Various Polymers

| copolymer | cell viability ^a (%) | | |
|---|---------------------------------|---------|----------|
| | N/P = 3 | N/P = 7 | N/P = 20 |
| PEI25K | 80 | 69.2 | 0 |
| PEI800 | 100 | 100 | 53 |
| PEI800- <i>g</i> -(PCL1200- <i>b</i> -PEG2000) _{1.4} | 99 | 96 | 51 |
| PEI25K- <i>g</i> -(PCL550- <i>b</i> -PEG550) ₂₁ | 98 | 100 | 46 |
| PEI25K- <i>g</i> -(PCL580- <i>b</i> -PEG5000) _{2.9} | 99 | 94 | 46 |
| PEI25K- <i>g</i> -(PCL1200- <i>b</i> -PEG2000) _{5.1} | 100 | 95 | 45 |
| PEI25K- <i>g</i> -(PCL2000- <i>b</i> -PEG2000) _{2.8} | 91 | 90 | 41 |

^a Calculated based on the protein level detected.

**Figure 8.** Transfection efficiency to 3T3 cells of polyplexes based on various copolymers.

(approximately 0 mV ξ -potential). As it is well-known that low ξ -potential correlates with low cytotoxicity, the polyplexes discussed here should be much more biocompatible than polyplexes on the basis of high molecular weight PEI. This notion was supported also by the cell viability during the transfection experiments (Table 3). At N/P ratios of 3 and 7, cells remained viable when transfected with complexes based on PEI800 Da and all copolymers. By contrast, cell viability dropped to 80% and 69%, respectively, when transfected with PEI25K-based polyplex. As N/P ratio reached 20, cells retained about 50% viability when transfected with PEI800 Da and copolymer-based polyplexes, whereas all cells were killed, i.e., protein amount detected is zero, when transfected with the polyplex of PEI25 kDa. More comprehensive cell culture experiment for assessing the biocompatibility of these complexes and their corresponding polymers is under way in our laboratory. The transfection efficiency to 3T3 cells with polyplexes based on various polymers is shown in Figure 8. At N/P 3, polyplexes based on PEI25 kDa, PEI25K-*g*-(PCL580-*b*-PEG5000)_{2.9}, and PEI25K-*g*-(PCL2000-*b*-PEG2000)_{2.8} may transfect the cells. Furthermore, polyplexes based on PEI25K-*g*-(PCL550-*b*-PEG550)₂₁ and PEI25K-*g*-(PCL1200-*b*-PEG2000)_{5.1} did not transfect the cells at all even at N/P 7, while they showed quite good transgene expression at N/P 20. In addition to their lower cytotoxicity (Table 3), at N/P ratios of 7 and 20, two polyplexes based on PEI25K-*g*-(PCL580-*b*-PEG5000)_{2.9} and PEI25K-*g*-(PCL2000-*b*-PEG2000)_{2.8} showed remarkable transfection efficiency. Only the polyplex based on PEI25 kDa may transfect the 3T3 cells more efficiently but seems to be very cytotoxic (Table 3). These

significant differences in gene transfection performance are obviously due to copolymer compositional variation.

As mentioned in the discussion of complex size and ξ -potential, the PEI head of PEI25K-*g*-(PCL1200-*b*-PEG2000)_{5.1} and PEI25K-*g*-(PCL550-*b*-PEG550)₂₁ is surrounded by dense hydrophobic PCL chains that may block or hinder the access and binding of hydrophilic DNA to PEI. In comparison with PEI25K-*g*-(PCL550-*b*-PEG550)₂₁, PEI25K-*g*-(PCL1200-*b*-PEG2000)_{5.1} formed smaller complexes (208 nm vs 335 nm). We speculate that, at N/P 3 and 7, PEI25K-*g*-(PCL1200-*b*-PEG2000)_{5.1} complexed the least amount of DNA. This is almost certain when recalling that the cmc of PEI25K-*g*-(PCL1200-*b*-PEG2000)_{5.1} is much lower than that of PEI25K-*g*-(PCL550-*b*-PEG550)₂₁, and complexation with DNA may lead to a further decrease of its cmc. Therefore, the insufficient transfection performance of PEI25K-*g*-(PCL1200-*b*-PEG2000)_{5.1} is likely due to its insufficient loading of DNA rather than the incomplete compaction and condensation of DNA that occurred with PEI800 Da and PEI25K-*g*-(PCL550-*b*-PEG550)₂₁. In this sense, not only the graft density but also the PCL block length will play a crucial role in the copolymer/DNA polyplex formation because the PCL length seems to have an even more significant effect on the cmc of the copolymer. For instance, copolymers based on PCL 3800 showed very poor solubility (Table 2). We have already demonstrated that the hydrogen bonding between PCL and PEI in the bulk sample strengthened with increasing amounts of PCL attached to PEI (Figure 6) and significantly affected the dissolution of the bulk copolymer in aqueous solution. We suggest that hydrogen bonding between PCL and PEI may possibly occur also in solution and affect the incorporation of DNA to PEI.

Conclusions

Novel biodegradable copolymers, *hy*-PEI-*g*-PCL-*b*-MPEGs, have been successfully synthesized, and their molecular structures and physicochemical properties were characterized. Their thermal properties and water solubility were found to be dependent on the copolymer composition (i.e., block length and graft density). A hydrogen bonding between the PCL and PEI blocks in bulk copolymers was verified with FTIR measurements and should be one of the main factors affecting the water dissociation and thermal properties of bulk copolymers. Our initial results indicate that DNA complexation/condensation and gene transfection efficiency strongly depend on the copolymer composition (i.e., block length and graft density). With composition control, a graft copolymer may show a good combination of high transfection efficiency and good compatibility. However, there is no evidence that the incorporation of the hydrophobic polyester segment may likely enhance cell interactions and permeability of complexes, resulting in improvement in gene transfection efficiency. Recalling that these copolymers possess an advantage over many gene transfer vectors already reported so far, i.e., their potential biodegradability, we can expect that some of these copolymers could be promising new vectors for gene delivery. Further studies on the biodegradation behavior, DNA binding stability, and nuclease resistance of these polyplexes under physiological conditions are under way in our laboratory. In addition, on the basis of these copolymers, we have successfully achieved a supramolecular device showing good solubility in aqueous solution, much enhanced DNA binding and

condensation, and consequently excellent transgene expression, comparable to high molecular weight PEI.

Acknowledgment. We thank the Deutsche Forschungsgemeinschaft (DFG) for financially supporting this research. X.S. is grateful to the Alexander von Humboldt Foundation (Germany) for a research fellowship.

References and Notes

- (1) Boussif, O.; Lezoualc'h, F.; Zanta, M. A.; Mergny, M. D.; Scherman, D.; Demeneix, B.; Behr, J. P. *Proc. Natl. Acad. Sci. U.S.A.* **1995**, *92*, 7297–7301.
- (2) Toncheva, V.; Wolfert, M. A.; Dash, P. R.; Oupicky, D.; Ulbrich, K.; Seymour, L. W.; Schacht, E. H. *Biochim. Biophys. Acta* **1998**, *1380*, 354–368.
- (3) Choi, Y. H.; Lui, F.; Kim, J. S.; Choi, Y. K.; Park, J. S.; Kim, S. W. *J. Controlled Release* **1998**, *54*, 39–48.
- (4) Lim, Y. B.; Kim, S. M.; Lee, Y.; Lee, W. K.; Yang, T. G.; Lee, M. J.; Suh, H.; Park, J. S. *J. Am. Chem. Soc.* **2001**, *123*, 2460–2461.
- (5) Kukowska-Latallo, J. F.; Bielinska, A. U.; Johnson, J.; Spindler, R.; Tomalia, D. A.; Baker, J. R. *Proc. Natl. Acad. Sci. U.S.A.* **1996**, *93*, 4897–4902.
- (6) Kabanov, V. A.; Sergeyev, V. G.; Pyshkina, O. A.; Zinchenko, A. A.; Bezin, A. B.; Joosten, J. G. H.; Brackman, J.; Yoshikawa, K. *Macromolecules* **2000**, *33*, 9587–9593.
- (7) Wolfert, M. A.; Schacht, E. H.; Tonceva, V.; Ulbrich, K.; Nazarova, O.; Seymour, L. W. *Hum. Gene Ther.* **1996**, *7*, 2123–2133.
- (8) Kataoka, K.; Togawa, H.; Harada, A.; Yasugi, K.; Matsumoto, T.; Katayose, S. *Macromolecules* **1996**, *29*, 8556–8557.
- (9) Kakizawa, Y.; Harada, A.; Kataoka, K. *Biomacromolecules* **2001**, *2*, 491–497.
- (10) Itaka, K.; Harada, A.; Nakamura, K.; Kawaguchi, H.; Kataoka, K. *Biomacromolecules* **2002**, *3*, 841–845.
- (11) Reviewed by Ledley, F. *Hum. Gene Ther.* **1995**, *6*, 1129–1144.
- (12) Behr, J. P. *Chimia* **1997**, *51*, 34–36.
- (13) Harpe, A. V.; Petersen, H.; Li, Y.; Kissel, T. *J. Controlled Release* **2000**, *69*, 309–322.
- (14) (a) Vinogradov, S. V.; Bronich, T. K.; Kabanov, A. V. *Bioconjugate Chem.* **1998**, *9*, 805–812. (b) Nguyen, H. K.; Lemieux, P.; Vinogradov, S. V.; Gebhart, C. L.; Guerin, N.; Paradis, G.; Bronich, T. K.; Alakhov, V. Y.; Kabanov, A. V. *Gene Ther.* **2000**, *7*, 126–138. (c) Ochietti, B.; Lemieux, P.; Kabanov, A. V.; Vinogradov, S.; St-Pierre, Y.; Alakhov, V. *Gene Ther.* **2002**, *9*, 939–945.
- (15) Bronich, T.; Kabanov, A. V.; Marky, L. A. *J. Phys. Chem. B* **2001**, *105*, 6042–6050.
- (16) Petersen, H.; Martin, A. L.; Stolnik, S.; Roberts, C. J.; Davies, M. C.; Kissel, T. *Macromolecules* **2002**, *35*, 9854–9856.
- (17) Petersen, H.; Fechner, P. M.; Fischer, D.; Kissel, T. *Macromolecules* **2002**, *35*, 6867–6874.
- (18) Petersen, H.; Fechner, P. M.; Martin, A. L.; Kunath, K.; Stolnik, S.; Roberts, C. J.; Fischer, D.; Davies, M. C.; Kissel, T. *Bioconjugate Chem.* **2002**, *13*, 845–854.
- (19) Petersen, H.; Kunath, K.; Martin, A. L.; Stolnik, S.; Roberts, C. J.; Davies, M. C.; Kissel, T. *Biomacromolecules* **2002**, *3*, 926–936.
- (20) Petersen, H.; Merdan, T.; Kunath, K.; Fischer, D.; Kissel, T. *Bioconjugate Chem.* **2002**, *13*, 812–821.
- (21) Batrakova, E. V.; Miller, D. W.; Li, S.; Alakhov, V. Y.; Kabanov, A. V.; Elmquist, W. F. *J. Pharmacol. Exp. Ther.* **2001**, *296*, 551–557.
- (22) Catherine, L. G.; Sriadibhatla, S.; Vinogradov, S.; Lemieux, P.; Alakhov, V.; Kabanov, A. V. *Bioconjugate Chem.* **2002**, *13*, 937–944.
- (23) Wang, D.; Narang, A. S.; Kotb, M.; Gaber, A. O.; Miller, D. D.; Kim, S. W.; Mahato, R. I. *Biomacromolecules* **2002**, *3*, 1197–1207.
- (24) Shuai, X.; He, Y.; Na, Y.; Inoue, Y. *J. Appl. Polym. Sci.* **2001**, *80*, 2600–2608.
- (25) Shuai, X.; Tan, H. *J. Appl. Polym. Sci.* **1997**, *66*, 1891–1898.
- (26) Shuai, X.; Jedlinski, Z.; Luo, Q.; Farhod, N. *Chin. J. Polym. Sci.* **2000**, *18*, 19–23.
- (27) Nathan, A.; Bolikal, D.; Vyavahare, N.; Zalipsky, S.; Kohn, J. *Macromolecules* **1992**, *25*, 4476–4484.
- (28) Veronese, F. M.; Saccà, B.; Polverino de Laureto, P.; Sergi, M.; Caliceti, P.; Schiavon, O.; Orsolini, P. *Bioconjugate Chem.* **2001**, *12*, 62–70.
- (29) Matsuzawa, Y.; Koyama, Y.; Hirano, K.; Kanbe, T.; Katsura, S.; Mizuno, A.; Yoshikawa, K. *J. Am. Chem. Soc.* **2000**, *122*, 2200–2205.
- (30) Weickenmeier, M.; Wenz, G. *Macromol. Rapid Commun.* **1997**, *18*, 1109–1115.
- (31) Hill, H. D.; Straka, J. G. *Anal. Biochem.* **1988**, *170*, 203–208.
- (32) Shuai, X.; Porbeni, F. E.; Wei, M.; Bullions, T.; Tonelli, A. E. *Macromolecules* **2002**, *35*, 3126–3132. Shuai, X.; Porbeni, F. E.; Wei, M.; Shin, I. D.; Tonelli, A. E. *Macromolecules* **2001**, *34*, 7355–7361.
- (33) Wei, M.; Tonelli, A. E. *Macromolecules* **2001**, *34*, 4061–4065.
- (34) Kurcok, P.; Dubois, P.; Sikorska, W.; Jedlinski, Z.; Jerome, R. *Macromolecules* **1997**, *30*, 5591–5595.
- (35) He, Y.; Li, J.; Shuai, X.; Inoue, Y. *Macromolecules* **2001**, *34*, 8166–8172.
- (36) Shuai, X.; Porbeni, F. E.; Wei, M.; Bullions, T.; Tonelli, A. E. *Macromolecules* **2002**, *35*, 2401–2405.
- (37) Shuai, X.; Porbeni, F. E.; Wei, M.; Bullions, T.; Tonelli, A. E. *Biomacromolecules* **2002**, *3*, 201–207.

MA034390W